GRID GENERATION USING CLASSICAL TECHNIQUES

Gino Moretti

Polytechnic Institute of New York
Farmingdale, N. Y. 11735

1. Historical

Conformal mapping has been used as a tool for solving problems in fluid mechanics and electromagnetism for more than one hundred years. Riemann's (somewhat incomplete) proof of the possibility of mapping closed contours on circles dates from 1850 [1]. Schwarz introduced what is now known as the Schwarz-Christoffel transformation in 1869 [2]. In the same year, Kirchhoff and Helmholtz used conformal mapping to solve classical problems of flows with free surfaces [3]. The importance of conformal mapping in fluid mechanics in the second half of the nineteenth century and the first quarter of the present one stems from the well-known property of invariance of the Laplace equation through conformal mapping; the mapping itself is, indeed, defined by a Laplace equation. Since the theory of images allows any incompressible, potential flow defined by given singularities to be determined in the presence of a circle or a straight line, the analogous problem in the presence of an arbitrarily given contour is reduced to the problem of mapping the contour onto a circle or a straight line. In so doing, the problem of determining the analytic function representing the complex flow potential is split into two parts. One consists of finding the potential for the circle, and that is easy. The other still requires the determination of an analytic function to define the mapping, which is as difficult a task as the original problem [4, page 77]. Nevertheless, it is much more appealing to people who have a visually oriented mind, and it can be subdivided in a number of successive steps, each one of which is easy to understand geometrically.

The Joukowski mapping,

$$z = \zeta + \frac{1}{\zeta} \tag{1}$$

discovered in 1910 [5], is extremely simple and easy to handle. Using a circle as the basic contour in the ζ-plane, it can generate a two-parameter family of cusped profiles and a three-parameter family of smooth contours ranging from familiar ellipses to peanut-shaped figures (Fig. 1). Despite their poor aerodynamical properties, the Joukowski profiles played a crucial role in the understanding of the mechanism of lift and, consequently, in the establishment of the theory of flight as a science. In creating his profiles, Joukowski introduced an idea which turned out to be extremely rich in consequences: that is, that a shifting of the center of the circle is sufficient to produce an airfoil having either camber or thickness or a combination of both.

Another major contribution dates from 1918 when von Kármán and Trefftz [6] observed that, if (1) is recast in the form:

$$\frac{z - 2}{z + 2} = (\frac{\zeta - 1}{\zeta + 1})^2 \tag{2}$$

it can be interpreted as a combination of two bilinear mappings and a power. If δ is used instead of 2 in (2), the Kármán-Trefftz mapping results:

$$\frac{z - \delta}{z + \delta} = (\frac{\zeta - 1}{\zeta + 1})^\delta \tag{3}$$

which, for $\delta = 2-\epsilon/\pi$, produces an airfoil with a finite internal angle, ϵ, at the trailing edge. The property of a power,

$$z = \zeta^\delta \tag{4}$$

to eliminate sharp corners, was known and had been applied since the times of Schwarz and Christoffel, but the importance of its application in (3) should not be underestimated.

The role played by the exponential (and, conversely, the logarithm) and by all functions directly related to it (direct and inverse trigonometric and hyperbolic functions) in generating infinite cascades can be traced back to König, 1922 [7]. Transformations of this kind, for example,

$$z = e^{i\beta} \log \frac{\zeta-\kappa}{\zeta+\kappa} + e^{-i\beta} \log \frac{\kappa\zeta-1}{\kappa\zeta+1} \tag{5}$$

have essential singularities at infinity. Therefore, the image
of the physical point at infinity in the plane of the circle is
generally a pair of spiral-vortices at a finite distance, a
geometrical property related to the ability of a cascade to de-
flect the flow.

Finally, in 1933 Ferrari found the basic mapping for bi-
planes. He showed that a doubly periodic function was needed,
that is, an elliptic function. His paper [8] is the first appli-
cation of elliptic functions to wing theory. [8].

Important as these basic mappings were, they did not
solve the problem of mapping an arbitrarily given contour onto a
circle. They generate a closed contour without sharp corners
which, in a favorable case, may look like a quasi-circular con-
tour which reminds one of a potato (the word "potato" has actual-
ly been used occasionally in the literature to designate such
figures and, although not defined in mathematical terms, seems to
be as acceptable as "quasi-circle"). The technique for the map-
ping of the quasi-circle onto a circle, proposed by Theodorsen in
1931 [9], actually brought conformal mapping from the speculative
level down to practical levels of aeronautical engineering. Its
basic idea is indeed extremely simple; if the center of the cir-
cle and the centroid of the quasi-circle are located in the ori-
gins of their respective planes, and some scaling is used to make
the areas of the two figures coincide, then the mapping can be
expressed in the form:

$$z = \zeta \, e^{f(\zeta)} \tag{6}$$

where $z=re^{i\phi}$, $\zeta=e^{i\theta}$ and the modulus of f is small. Therefore,
two equations follow:

$$\ln r = A(\theta) \quad , \quad \phi-\theta = B(\theta) \tag{7}$$

if $f = A + iB$. On the circle, A and B are conjugate Fourier
series. If ln r were known as a function of θ, A could be deter-
mined by expanding ln r into a Fourier series, and B would follow
automatically. Since ln r is known, instead, as a function of φ,
iterations are necessary to make the two equations compatible.
Alternatively, values of φ-θ can be obtained rephrasing the prob-
lem as an integral equation, so that the formula to be solved by
iteration is the Poisson integral:

$$\phi - \theta = \frac{1}{2\pi} \int_0^{2\pi} \ln r \cot \frac{\omega - \theta}{2} \, d\omega$$

<div align="right">(8)</div>

Convergence of the procedure is assured if the potato is "star-shaped", that is, if its contour is crossed only once by any radius issued from the center [10]; therefore, the procedure is generally safe and efficient.

Applications of the Theodorsen method to airfoils, biplanes and cascades were pioneered by Garrick [11,12,13], who used the transformations introduced by Joukowski, Ferrari and König to produce quasi-circles as intermediate images of given contours.

For a better understanding of the rest of this paper, three points should be made.
1) Mapping of a contour into an <u>exact</u> circle was necessary, when problems of incompressible, potential flow had to be solved, in order to take full advantage of the invariance of the Laplace equation and of the easy evaluation of the flow past a circle.
2) Since the only values of interest belonged to the rigid contours, all calculations could be limited to the circumference of the circle.
3) Nevertheless, all calculations, with the exception of the ones related to the Joukowski mapping, were extremely cumbersome when performed by hand. Most of the time, the Joukowski mapping was preferred to the Kármán-Trefftz mapping. Cascade and biplane problems were rather analyzed by approximate methods. The Hilbert integral, with the entire circumference subdivided in just a dozen intervals, was preferred to the more laborious Fourier expansions.

Such practical difficulties and the shifting of interest towards problems in compressible flow contributed to relegate conformal mapping into the background in the forties. When computers came about, there was not so much a demand for solution of incompressible, potential flow problems, and the consequent application of conformal mapping techniques.

4

2. Conformal mapping as a grid generator

Nevertheless, in recent times conformal mapping has again been looked upon in connection with problems of compressible flow, but of course the use of it as a device to solve the same equations of motion in a simpler plane has been dropped, since neither the Euler equations nor the Navier-Stokes equations are invariant by conformal mapping. The reason for revival stems from the fact that in contemporary numerical gas dynamics the equations of motion must be solved in the entire flow field, because of compressibility effects, viscous effects, presence of vorticity, etc. Contrariwise, for incompressible, potential flow it is theoretically correct and practically convenient to search for the solution on the rigid contour only. A computational grid is necessary, upon which the equations are to be discretized. When two space-like variables are involved, conformal mapping is a very convenient tool to generate a computational grid.

If the boundaries of the flow field are mapped onto a circle centered at the origin of a complex plane $\zeta = \rho e^{i\theta}$, the network of ρ=constant and θ=constant lines is conversely mapped onto the physical plane as an orthogonal grid, well draped around the rigid contours because the latter are the image of the circle itself.

Since the grid is orthogonal, the vector operators in the physical plane can be expressed directly and easily in terms of their counterparts in the mapped plane.

The search for an appropriate mapping is actually a search for a single function of a complex variable, a task by far simpler than the search for two functions of two independent variables. All the findings of more than a century, properly digested and interpreted as briefly shown in Section 1, can be put together to suggest the most appropriate mapping for a particular task. Our computers have eliminated the tediousness, inaccuracy and material errors which used to hamper the hand calculations of half a century ago; they also allow the necessary

data for a very refined grid to be evaluated in a fraction of a second. Complex arithmetic in FORTRAN and other languages of the same level reduces coding to just about a rewriting of the basic equations (except when angles contained in more than one quadrant are involved).

Practical applications of conformal mappings to generate grids have been developed in the last decade following two separate lines. One proceeds from the observation that any conformal mapping is defined by an analytic function, and that real and imaginary parts of the latter are harmonic functions. Therefore, the conformal mapping problem consists of solving two Laplace equations. The task can be formulated in strictly numerical terms, using modern, fast Laplace solvers. This viewpoint can be traced back to 1923 [14] and has been made popular by a 1975 paper by Thompson et al. [15]. The other puts the emphasis on the use of closed form analytical expressions for the mapping functions. It seems that the first non-airfoil related application of the technique was presented in 1972 [16], although the same problem was reformulated in a more general form only in 1974 [17]. We will try to analyze here the philosophy of the approach and to show how it works in practical cases.

3. Philosophy of the 'closed form' approach

We will begin by discussing some of the advantages of a closed form approach. To fully appreciate them, let us focus our attention on what the majority of problems of current interest are: Two-dimensional, unsteady flows or three-dimensional, steady flows. In the former, the physical space is two-dimensional but the computational grid may be variable in time; in these cases we need a grid, generated by conformal mapping at every instant of time, but depending on parameters which are functions of time. In the latter, we may find it convenient to create a computational grid on planes defined by two of the three space coordinates, and again letting the grid change as a function of the third coordinate. To organize the following formulae, let us stipulate that the Cartesian coordinates on any plane to be mapped are x and y, and that a complex coordinate is defined,

6

$$z = x + i y \qquad (9)$$

using the symbol t either for time or for the third space coordinate. The mapping of each z-plane onto another complex plane, defined by a variable ζ, will then be accomplished by an analytic function:

$$\zeta = \zeta(z;c) \qquad (10)$$

where c is shorthand for any parameter, function of t.

As in every flow problem, it is not so much the coordinate of a point as the derivatives at that point which matter. First, we need the derivatives of the coordinates in the physical plane with respect to the coordinates in the mapped plane, and vice versa, contained in the complex expression:

$$g = \frac{d\zeta}{dz} \qquad (11)$$

Then, we need second derivatives, which appear in dealing with the curl of the velocity vector, and these entail dg/dz. Finally, we need derivatives with respect to t, viz. $\partial\zeta/\partial t$ and $\partial g/\partial t$, which are computed from (10) and (11) by differentiating with respect to c and keeping z constant. Obviously, it is very convenient to have the mapping expressed in a closed analytical form since all derivatives are also expressed in closed form and can be exactly evaluated where and only where they are needed, that is, at the computational nodes. The argument is particularly interesting with regards to the t-derivatives. If the grid changes in t, the values of z generally change in t at each nodal point; therefore, numerical differentiation at a constant z may be cumbersome and inaccurate.

There is another case where having a closed form mapping is convenient. Potential (but not incompressible) flow problems, with the flow field extending to infinity, are commonly solved by relaxation. Commonly, the physical potential is expressed as the sum of an unknown and the potential of a flow, satisfying the proper physical conditions at infinity. The latter is easily formulated in terms of the transformed variables if the mapping

is defined by a closed form function.

Then, a difficulty seems to arise. As we said in Section 1, in most cases it is not possible to find a closed form mapping which provides an exact circle as the image of a given contour; it is clear that Theodorsen's step is not a closed form function. Nevertheless, the difficulty is only apparent. Let us assume, indeed, that we know a function capable of transforming a given contour into a quasi-circular potato. Let us consider a computational plane with two variables, X and Y, relating X to ρ and Y to θ. The functions $X(\rho)$ and $Y(\theta)$ will be so defined that X=0, Y=0, X=1 and Y=1 on each boundary, in turn. The computational region in the (X, Y) plane is, thus, the interior of a square. In most cases, the functions $X(\rho)$ and $Y(\theta)$ are used to apply proper stretching of coordinates in either direction, in order to concentrate nodes where necessary. The computational grid is orthogonal and divided into equal intervals. The corresponding grid in the ζ-plane is not orthogonal (not only because the X=0 line is not an exact circle, but also because the other boundaries may not be circles or straight lines either). Consequently, the grid in the physical plane is not orthogonal. Accuracy, however, is not impaired for want of orthogonality. The equations, originally written in the (ρ,θ) frame, are recast using X and Y as independent variables. Some additional terms will appear; the very important boundary condition on the rigid surface will be properly written by stating that the normal velocity component (not just the ρ-component) vanishes. In conclusion, we are not expecting any dramatic advantage from having a circle as one of the boundaries, and therefore we may consider our mapping problem solved when we find a quasi-circle as the mapped image of the given boundary. The Theodorsen step can be dropped with all its additional burden of iterations, Fourier expansions, spline fittings, etc.

Let it be clearly stated that we are not afraid of unsurmountable difficulties or unaffordable computational times connected with the Theodorsen step. That old (but hard to execute by hand) way of computing Fourier expansions, which has been given a new popularity under the FFT label serves the purpose egregiously well. Dropping the Theodorsen step, whenever possible, is justified by our desire of achieving a solution to the problem in a closed form, with a view to the formal calculation

of derivatives, particularly with respect to t. There is a definitive need for them in all problems where the grid depends on t.

This philosophy was clearly exposed in [16] and accepted by Jameson [18,19]. We will discuss some applications in Sections 5 through 8. Before that, we will mention some of the techniques which we tend to classify as numerical, rather than analytical.

4. Conformal mapping as a Neumann problem

The closed form approach may look like an empirical attempt to solve the problem, on the basis of analogies and imaginative variations, and therefore strongly dependent on the mental structure of the investigator. I have heard the word "art" used in a derogatory sense in connection with this type of work, on other occasions. Actually, good science is the product of personal ingenuity and crafty skill. What tends to be classified as "scientific" in these days is rather "technological", that is, some process which has been sealed in a black box for general purposes.

Whatever the consequences, there is no doubt that the quest for an organized conformal mapping procedure is legitimate. It is also classical. Green's formula:

$$\oint (u \frac{\partial v}{\partial n} - v \frac{\partial u}{\partial n})ds = 0 \tag{12}$$

for two harmonic functions, u and v, regular in the domain surrounded by the closed contour on which the integral is made, and on the contour itself, dates from 1828. With any two points on the contour denoted by $\zeta = \rho e^{i\theta}$ and $z = r e^{i\phi}$, and with $\zeta - z = \sigma e^{i\alpha}$, it follows from (12) that

$$u(z) = - \frac{1}{\pi} \oint [u(\zeta) \frac{\partial \ln \sigma}{\partial n} - \frac{\partial u}{\partial n} \ln \sigma] ds \tag{13}$$

All formulae related to conformal mappings can be obtained from (13); $\partial u/\partial n$ is generally known from its conjugate, the variation

of the tangent along the contour. Then (13) becomes an integral
equation for u.

Many different forms of the equation can be obtained, if
one makes use of well-known properties and formal rules, such as:
the Cauchy-Riemann conditions, integration by parts, Schwarz and
Poisson's integrals, integrals defining the coefficients of a
Laurent series. Different forms are also obtained by taking the
basic contour as a circle or as a straight line, and by defining
u either as the logarithm of z or as the logarithm of g. For ex-
ample, if we start from (6) and from a circle, the other contour
being a quasi-circle, we obtain the Theodorsen mapping in its in-
tegral form (8); the Fourier series form follows easily. The same
equation (6) and somewhat different integral equations have been
used by Symm [20] and Hayes et al. [21] to produce numerical
techniques which are not restricted to mappings of quasi-circles
onto circles, as in Theodorsen's, but apparently can handle any
(probably, star-shaped) contour. If we use the logarithm of g,
we can interpret Theodorsen's ideas in terms of derivatives, á la
Timman [22], a variation which seems to offer some numerical ad-
vantages [17].   If we start from a straight line and an arbi-
trary, closed contour, using again the logarithm of g, we obtain
what Davis [23] presents as a generalization of the Schwarz-
Christoffel mapping to a polygon with an infinite number of in-
finitesimal vertices:

$$\log g = \frac{1}{\pi} \int \log (\zeta - b)\ d\beta \qquad\qquad (14)$$

Anyone interested in these types of comparisons could profitably
read a paper by Birkhoff et al. [24] which is outdated only from
a computational viewpoint.

Proceeding in the opposite direction as Davis, the
Schwarz-Christoffel formula for a polygon with a finite number of
vertices can be found as a particular case of (14). This formula
is, in principle, a very powerful mapping tool. It can map a po-
lygon on a circle, without restricting number, location and aper-
ture of vertices, or the lengths of the sides, and permitting
vertices to be located at infinity. It is really a definition of
g, rather than of ζ, which must be obtained by complex integra-
tion in a numerical form, in almost all the cases. This is not a
major shortcoming, however, since numerical integration can be

performed quickly and efficiently. The derivative, dg/dz is
straightforward. Nevertheless, it is known that the coeffi-
cients, ζ_i and δ_i which appear in the formula

$$g = \Pi \ (\zeta - \zeta_i)^{\delta_i} \tag{12}$$

must be obtained by trial-and-error iterative processes (see, for
example, [23,25,26]). If the grid does not depend on t, its
coefficients can be determined once and for all. In this case
the Schwarz-Christoffel formula belongs to the category which we
consider in the present paper. It does not if the grid depends
on t. The same may be said for all mappings obtained by solving
a Neumann problem via iterations on an integral equation or
Fourier expansions.

5. Kármán-Trefftz mapping for airplane cross sections

We will now consider some mappings using a finite number
of closed form relations.

The numerical analysis of a steady, supersonic flow past
an airplane may be performed by marching in an axial direction
and updating values at successive cross-sectional planes. The
region of interest in each plane is bounded by the section of the
body and the section of the bow shock. Conformal mapping of the
body onto a quasi-circular shape provides a grid which tends to
become a polar grid at infinity and therefore is the best suited
to adjust to the shape of the body, whatever it is, and to the
almost circular shape of the bow shock. The body shows a number
of edges and corners as those indicated by letters in Fig. 2. If
the airplane is arrow-winged, stations will be reached where the
body will be composed of three unconnected parts; if two ficti-
tious lines are drawn between the fuselage and the trailing edges
of the wings, again we can see corners and edges at all points
denoted by letters in Fig. 3. Observing that the corners and
edges always come in pairs, because of the symmetry of the cross-
section, we can think of eliminating them by successive applica-
tions of the Kármán-Trefftz mapping (3), with the singular points

either on the contour or, in case of rounded edges and corners, slightly inside. Note that edges require values of δ between 1 and 2 and corners require values of δ less than 1. When the latter are applied, the corner is open, but so is the rest of the plane, part of which may end up in a second Riemann sheet. In principle, this is not an obstacle to the removal of corners, because the portion of plane which disappeared will be recalled when removing the next edge. In practice, a quite cumbersome additional piece of logic must be added to identify points belonging to the second Riemann sheet. The trouble can be avoided by executing the mappings not according to the order of appearance of a corner or edge along the contour but in a sequence of decreasing values of δ.

From the viewpoint of coding, the repeated application of the Kárman-Trefftz procedure has many advantages:
1) Regardless of the number, position and aperture of corners and edges, the same operation is used, which means the code may be written in the form of a loop and applied as many times as necessary, automatically,
2) The mapping can be inverted, and the inverse mapping has the same form; therefore, the same routine can be used for the direct and the inverse mapping,
3) The derivatives are easily coded; for example g, as defined by (11), is actually the product of the derivatives of each intermediate step, and the logarithmic derivative of g is the sum of the logarithmic derivatives of such steps.

To show how close to a circle the image of a fuselage with two sections of arrow wings is, Fig. 4 presents a computational grid in the physical plane and its image in the mapped plane. Naturally, with the bow shock very close to the leading edge of the wings, its own image is far from a circular shape but, as we said above, departure from orthogonality of the grid is not jeopardizing accuracy, and this is particularly true in the vicinity of the bow shock, where the flow is uncomplicated. Details of the technique and its application to the arrow-winged airplane problem can be found in [17].

6. Imaginative devices

There are no limits to the number of shapes which can be obtained by executing elementary mappings in a sequence and using a little ingenuity. Indeed, bilinear transformations, powers and logarithms are the building blocks with which one should learn to play, always keeping in mind that rotations and translations can be cleverly used to locate singularities where needed. Here is an interesting example, due to Rossow [27], which is entirely expressible by a sequence of bilinear mappings and powers (Fig. 5).

A circle, centered at the origin, is translated upwards and then a Joukowski mapping changes it into an arc of a circle, counted twice. The arc is rotated about one of its ends and a new singular point is defined somewhere along its length. A new Joukowski mapping is applied, in reverse, so that the portion of the arc between the two singular points become a circle again, and the portion left outside remains appended like an infinitely thin tail. Finally the circle is relocated, and a third Joukowski mapping is used to transform it into a Joukowski profile; the little tail becomes a flap or spoiler, whose location and length can be controlled by changing the parameters used in the successive steps. According to our quasi-circular philosophy, this very simple mapping can be used for any airfoil with attached (but not infinitely thin) spoilers or flaps.

I faced a similar problem when confronted with generating a grid for the calculation of the precursor muzzle blast [28]. I needed a grid shaped as in Fig. 6; the contour defined by D'C'CD can be mapped onto the real axis of a w-plane, and its exterior onto the upper half w-plane by a simple Schwarz-Christoffel transformation [29, page 159], but this mapping would not provide a family of grid lines issuing from what has to be interpreted as the bore of the gun and wrap around the barrel, as in the figure. The problem was solved by defining two new singular points, B and B', in the w-plane and applying to this plane an inverse Joukowski mapping onto a ζ-plane. Radial straight lines and concentric circles in the ζ-plane are now producing the wanted grid

in the z-plane. Note that the position of B and B', being arbi-
trary, permits the ratio of outer-to-inner radius of the barrel
to be matched (Fig. 7). With the change of notation: w = Z +
1/Z, which simplifies the coding, the mapping is thus defined by:

$$z = (r_o/\pi)[(Z^2-1/Z^2)/2 = \log Z^2 - i\pi]$$

(15)

$$Z + 1/Z = 2 B (\zeta + 1/\zeta)$$

In the problem just described, the computational region
is limited, on one side, by the precursor shock which moves out
in time. Therefore, the computational grid is a function of
time, but the dependence on time shows only through the stretch-
ing parameters; the mapping itself remains invariable in time and
the equations of motion carry no terms of the type $\partial g/\partial t$ or
$\partial \zeta/\partial t$. When a mapping is needed for the same problem in the
presence of a protruding bullet, however, the contour itself
changes in time and so does the mapping. Once more, the problem
can be solved with little additional effort. One can start with
a half circle (Fig. 8), reduce it to a half ellipse using a
Joukowski mapping, and then apply a Kármán-Trefftz formula to
change the angles between the contour and the real axis. After
that, the mapping continues as defined by (15). The axis ratio
of the ellipse keeps growing as the bullet nose advances. The
power in the Kármán-Trefftz mapping decreases from an initial 1
to a minimum value of 1/2. At this stage, the contour in the
physical plane makes a 90 degree turn at B and B', as required to
accomodate the grid to the side surface of the bullet (Fig. 9).

7. Different mappings for the same geometry

In solving problems of incompressible, potential flow
there is no ambiguity about the choice of the mapping since the
contours of interest are specified exactly and the mapping func-
tion has to be regular over the entire flow field (boundaries ex-
cluded). In the present context, though, different mappings may
accomodate the same contours but generate completely different
grids, as we have mentioned in the preceding Section. Care must
be taken to use a mapping whose grid is the best suited for the

14

problem in hand. This problem is currently acute in cascade analysis, as we will mention later; here I would like to show it in a simpler connection.

We want to generate a grid for the intake of which Fig. 10 shows the centerline and the shroud. We can drape our grid about a semi-infinite slit, parallel to the real axis in the upper half-plane. Two mapping functions, apparently opposed to one another, can serve the purpose. The first is:

$$z = \zeta + e^{\zeta} \tag{16}$$

This function maps the slotted half plane onto a strip, which is a very convenient domain for our computational variables X and Y. The corresponding grid (Fig. 11) is convenient for the interior of the intake, but it needs some stretching to provide resolution to the exterior of it; in particular, the outer surface of the shroud is poorly resolved. The other mapping is defined by:

$$z = \zeta + a \log \zeta \tag{17}$$

and it maps the same region of the physical plane onto the entire upper ζ-half-plane. Cartesian coordinates in the ζ-plane produce the grid of Fig. 12. In this case, the grid is very good outside and very poor inside. If we start from polar coordinates in the ζ-plane, we obtain the grid of Fig. 13. The general appearance of the grid lines recalls Fig. 11, but the situation is reversed: the resolution is very poor inside and very good outside; in this case, an accumulation of ρ=constant lines near the origin of the ζ-plane is necessary to generate some coordinate lines inside the intake. An application of (16), with a stretching of coordinates to relax the resolution inside the nacelle, has been made by Caughey and Jameson [30].

Anyway, these mappings are obtained in a very straightforward manner, and more complicated manipulations [31] do not seem necessary.

8. Biplanes, revisited

Ives [32] has proposed a technique for the mapping of two airfoils which is rich in possible consequences. We have seen in Section 5 how the successive application of Kármán-Trefftz mappings can eliminate corners and edges on a contour, producing a quasi-circular shape. A similar idea, exploiting the theory of images with respect to a circle, allows two airfoils to be mapped on two concentric circles. Two Theodorsen mappings are used as intermediate steps, as follows (Fig. 14). First, a Kármán-Trefftz formula is applied to transform one of the airfoils into a quasi-circle, and then the quasi-circle is transformed into an exact circle by the Theodorsen technique. At this stage, the second airfoil is still shaped as an airfoil although with a different shape. The next step manages to transform the second airfoil into a quasi-circle, without distorting the first circle. The problem is solved by using the product, side-by-side, of two Kármán-Trefftz formulae; the first contains the two singular points pertinent to the second airfoil (a and b) and their counterparts in the mapped plane (α and β); the second contains the images of such points ($1/a^*, 1/b^*$ and $r_o^2/\alpha^*, r_o^2/\beta^*$, respectively, where conjugates are denoted by * and r_o is the radius the image of the first circle in the mapped plane):

$$
\frac{(\zeta-\alpha)(\zeta-r_o^2/\alpha^*)}{(\zeta-\beta)(\zeta-r_o^2/\beta^*)} = [\frac{(z-a)(z-1/a^*)}{(z-b)(z-1/b^*)}]^\delta
\tag{18}
$$

Finally, the second quasi-circle is moved inside the first circle by a bilinear transformation in such a way that its centroid coincides with the center of the circle, and a second mapping of the Theodorsen type is applied. Again, such a mapping must take into account that the flow region is a ring between two concentric circles. Therefore, the exponent in (6) cannot be a simple Taylor series, as it would be if the flow occurred inside a circle, or a Taylor series of negative powers, as it would be if the flow occurred outside a circle, but it must be a two-sided Laurent series; we express this need by saying that the Theodor-

sen mapping is defined in this case by:

$$z = \zeta \, e^{f(\zeta;c)-f(1/\zeta;c^*)} \qquad (19)$$

where c is any constant occurring in $f(\zeta)$ [12].

The idea of using the images of the singularities with respect to a circle in order to operate on the other contour without distorting the circle can surely be extended to problems dealing with two separate contours but not necessarily airfoils.

Two questions can be posed. First, how can Ives' technique produce the mapping, without using elliptic functions? The explanation can be found in the fact that the sequence of mappings used by Ferrari and Garrick consists of a logarithm, followed by an elliptic function. The net result actually has only one period, the other being neutralized by the multi-valuedness of the logarithm. On the other hand, the periodicity is introduced in Ives' mapping through the play of reflections of singularities produced by (19). The second question is whether one could bypass the two Theodorsen corrections, in the spirit of Section 3 above. Of course, in this case we would have to deal not with one distorted circle alone, but two, the first being particularly important since the images of (19) would, in any case, be defined with respect to a circle which now would only be an approximation to the real contour. I believe that the technique could still be applied, but no examples are available.

9. Cascades

The climax of difficulties is reached in the problem of generating a grid to compute flows through a cascade of airfoils. Garrick [13] sensed the difficulty well ahead of the computer era, but he did not have a way of measuring it; as we said, hand computations were necessarily limited to the simplest cases. He said: "It is to be noticed that improvements in the initial transformation are desirable and should be sought, particularly to take care of highly cambered airfoils more conveniently, in

order to reduce the amount of subsequent calculations." At that
time, the initial transformation was the one defined by (5), ob-
viously a poor way to get started when dealing when highly cam-
bered airfoils, since the basic shape furnished by (5) is a cas-
cade of flat, straight, double-sided segments. Unfortunately, in
a cascade four parameters must be considered, solidity, stagger,
camber and thickness, and these parameters interact with each
other, whatever the choice of the basic mapping. So long as
solidity and stagger are low, even (5), applied to a moderately
thick and cambered airfoil, produces a reasonable quasi-circle.
But as solidity and stagger increase, the contour tends to become
peanut-shaped (Fig. 15), with a catastrophic distribution of
points around it (something like a wide circle, corresponding to
a small portion of the original profile, with a small appendix,
which is the image of all the rest); and, at times, the contour
is not even star-shaped any longer. Can (5) be blamed for such a
behavior? A detailed discussion of this question would transcend
the limits of the present paper; let it just be said that the
difficulty does not disappear when another mapping function,
adopted by Legendre [33] and Ives [34], is used (Ives' function
is the same as Legendre, to within a rotation and a bilinear
transformation). This mapping can be written in the form:

$$[\frac{\zeta + b}{\zeta - b}]^{\delta} = \frac{\sin A(z - 1)}{\sin A(z + 1)} \tag{20}$$

where z and ζ are the physical plane and the mapped plane,
respectively, 1 and -1 are the location of the trailing edge and
the center of the leading edge of a profile, respectively, δ is
the usual Kármán-Trefftz exponent, A is related to solidity and
stagger by

$$2 i A = \pi s e^{i\beta} \tag{21}$$

and

$$b = - i \tan \frac{A}{\delta} \tag{22}$$

So far, the major advantages of this transformation with respect
to (5) are the presence of an exponent, δ to produce profiles
with a finite trailing edge angle, and the possibility of comput-
ing either ζ as a function of z, directly from (20), or z as a
function of ζ from the inverse of (20):

$$z = -1 - \frac{i}{2A} \log \frac{e^{2iA} - w^{\delta}}{e^{-2iA} - w^{\delta}} \qquad (23)$$

with

$$w = \frac{\zeta + b}{\zeta - b} \qquad (24)$$

When stagger and solidity are high, most of the skill which must be used to follow the contour properly in applying (20) is wasted, due to the ungainly shape of the resulting contour. More manipulations are needed before a quasi-circular shape is obtained; but we will not elaborate on this point in the present paper.

Let us assume then, that a circle has been obtained somehow from the given cascade; and, in the spirit of Section 3, we will gladly accept a quasi-circle, without refining the mapping any further. At this stage, we must decide what type of grid we want. Different choices can indeed be made for the general appearance of the grid. Three of these are the most common (Fig. 16). The first contains lines which run from left to right through the cascade, more or less as streamlines of a real flow would do. The second (commonly called an O-grid) contains lines wrapped around each profile. The third (commonly called a C-grid) contains similar lines which run around the profile and an infinite line issuing from the trailing edge, as a wake. Now, regardless of the choice of the first mapping step, the plane of the circle will always have four singular points, representing the points at infinity (on the left and the right of the cascade) and their reflections on the circle. If we invert the circle plane so that the interior of the circle corresponds to the exterior of the cascade, then the two singular points inside the circle represent the physical points at infinity. A system of streamlines and equipotential lines for an incompressible, potential flow, proceeding from one singular point to the other and having stagnation points at the points on the circumference which correspond to the leading and trailing edge, provides a grid of the first type. In building it up, one finds numerical difficulties. It is indeed hard to follow a streamline on a spiral vortex when the singular point is very close to the periphery of the circle (this is what happens with high solidity and high

stagger).

Polar coordinates are very simple to use, but they generate a very inconvenient grid because of the presence of a singularity in the flow field between profiles, at the point corresponding to the center of the circle [35]. (See Fig. 17.)

For an O-grid, the best procedure has been suggested by Ives [35]. It consists of mapping the circle onto a rectangle, in such a way that two vertices correspond to the singular points (points at infinity in the physical plane) and the opposite side corresponds to the circumference (the contour of the profile). The basic function defines the correspondence shown in Fig. 18 (where there is a straight slit between the two singularities). In the same figure, lines corresponding to straight lines, parallel to the sides of the rectangle, are shown inside the circle. The function which performs the task is the simplest of the Jacobian elliptic functions:

$$z = \text{sn} (\zeta, m) \qquad (25)$$

where m is defined by the position of the singularities and tends to 1 when solidity and stagger increase. Using Landen's transformations, the sine-amplitude can be expressed in terms of trigonometric functions (for m close to 0) or the hyperbolic tangent (for m close to 1); the coding of the subroutine is obvious and the computational time is negligible. Therefore, (25) is a convenient function.

Note that the circle (or quasi-circle) obtained through (5) or (20), and the circle obtained from (25) are by no means the same, despite the fact that in both planes the images of the points at infinity are symmetrically located on the real axis. The second circle is centered at the origin, but the first is not; therefore, a bilinear transformation must be used to map the two circles onto each other. This mapping depends on all four basic parameters and the trailing edge angle as well. Its interpretation, thus, is not easy, but a systematic study is needed to understand what range of basic contours, acceptable as a background of a grid for given profiles, can be obtained by using (25), a bilinear mapping and (23), in that sequence, without resorting to a Theodorsen step. It seems to me that we either

have reasonable shapes, in which case that step can be skipped, or combinations of solidity and stagger which tend to generate intermediate shapes similar to the one on the right hand side of Fig. 15, in which case the Theodorsen technique would not work, and where another intermediate step, of a different nature, should be used. Even Joukowski mappings may help (see the last contour in Fig. 1). Work along these lines is urgently needed, if we want to obtain simple mapping procedures for three-dimensional turbomachinery problems. To make the point, we present a three-step sequence, in which the first circle, obtained from the rectangle, is the one of Fig. 18. A second circle (Fig. 19) is obtained by a bilinear transformation and the cascade, obtained through (23) is shown in Fig. 20. The contour is ugly, but the grid is perfectly usable.

10. Grids for ablated, three-dimensional bodies

We conclude this presentation showing a method applied to generate a computational grid for a three-dimensional, time-dependent problem. The flow to be determined is the shock layer around the ablated nose of a cone-cylinder; the flow is mostly supersonic, but it may have a subsonic bubble and an imbedded shock. The geometry of the body, which is axisymmetrical before ablation, becomes three-dimensional because of different ablation in different meridional planes. A grid is needed in a number of these planes, and corresponding points must be connected between adjacent planes, in order to generate a three-dimensional computational mesh. It is therefore convenient to have a grid defined in closed form, to make the evaluation of circumferential derivatives as easy as possible. For a given section of the body (Fig. 21) we define a skeleton, that is, a polygon, all contained inside the body, approximating the shape of the wall. Instead of using a Schwarz-Christoffel function to transform the skeleton into a straight line in a single operation, we have opted for straightening one vertex of the polygon at a time, beginning with the one farther from the nosetip. As in the case of the repeated Kármán-Trefftz mappings, the procedure is easily coded in a loop. The last step consists of a square root transformation, in order to bring the skeleton on the real axis and the body axis on the

imaginary axis of the ζ-plane. The image of the wall on the ζ-plane is close to a straight line. The grid, which will be normalized between the image of the wall and the image of the bow shock, is always well shaped, despite strong concavities of the body produced by severe ablation. The method, first tested on axisymmetric problems [37], has been successfully applied to three-dimensional problems [38].

11. References

1. B. Riemann, Grundlagen für eine allgemeine Theorie der Functionen einer veränderlichen complexen Grösse, in "Collected works of Bernhard Riemann", Dover Publ., New York 1953.

2. H.A. Schwarz, Gesammelte Abhandlungen, Berlin 1890.

3. G.R. Kirchhoff, Zur Theorie freier Flüssigkeitsstrahlen, in "Gesammelte Abhandlungen", Leipzig 1881.

4. H. Lamb, Hydrodynamics, Dover Publ., New York 1945.

5. N. Joukowski, Ueber die Konturen der Drachenflieger, ZFM 1910.

6. T. von Kármán and E. Trefftz, Potentialströmungen um gegebene Tragflächen-Querschnitte, ZFM 1918.

7. E. König, Potentialströmung durch Gitter, ZAMM $\underline{2}$, 422, 1922.

8. C. Ferrari, Sulla trasformazione conforme di due cerchi in due profili alari, Mem. Acc. Sci. Torino (2), $\underline{67}$, 1933.

9. T. Theodorsen, Theory of wing sections of arbitrary shape, N.A.C.A. TR 411, 1931.

10. S.E. Warschawski, On Theodorsen's method of conformal mapping on nearly circular regions, Quart. Appl. Math., $\underline{3}$, 12, 1945.

11. T. Theodorsen and I.E. Garrick, General potential theory of arbitrary wing sections, N.A.C.A. TR 452, 1933.

12. I.E. Garrick, Potential flow about arbitrary biplane wing sections, N.A.C.A. TR 542, 1936.

13. I.E. Garrick, Conformal mapping in Aerodynamics, with emphasis on the method of successive conjugates, Symp. on construct. and appl. of conf. maps., Nat. Bureau of Standards, Appl. Math. Series $\underline{18}$, 137, 1949.

14. H.B. Phillips and N. Wiener, Nets and the Dirichlet problem, J.Math.Phys. $\underline{2}$, 105, 1923.

15. J.F. Thompson, F.C. Thames, C.W. Martin and S.P. Shanks, Use of numerically generated body-fitted coordinate systems for solution of the Navier-Stokes equations, Proc. AIAA 2nd Comp. Fl. Dyn. Conf., 10, 1975.

16. G. Moretti, B. Grossman and F. Marconi, Jr., A complete numerical technique for the calculation of three-dimensional inviscid supersonic flows, AIAA Paper 72-192, 1972.

17. G. Moretti, Conformal mappings for computations of steady, three-dimensional, supersonic flows, Numerical/Laboratory Comp. Methods in Fl. Mech., ASME, 13, 1976.

18. A. Jameson, Iterative solution of transonic flows over airfoils and wings, including flows at Mach 1, Comm. Pure Appl. Math. 27, 283, 1974.

19. D.A. Caughey, A systematic procedure for generating useful conformal mappings, Int. J. Num. Meth. in Eng., 12, 1651, 1978.

20. G.T. Symm, An integral equation method in conformal mapping, Numer. Math. 9, 250, 1966.

21. J.K. Hayes, D.K. Kahaner and R.G. Kellner, An improved method for numerical conformal mapping, Math. of Comp. 26, 327, 1972.

22. J.L. van Ingen, Advanced computer technology in aerodynamics, AGARD LS 16, 1969.

23. R.T. Davis, Numerical methods for coordinate generation based on Schwarz-Christoffel transformations, AIAA Comp.F.Dyn.Conf., Williamsburg, Va. 1979, page 180.

24. G. Birkhoff, D.M. Young and E.H. Zarantonello, Numerical methods in conformal mapping, Proc. Symp. in Appl. Math., vol. 4, Fl. Dyn, McGraw-Hill, Publ. 1953, page 117.

25. R.S. Skulsky, A conformal mapping method to predict low-speed aerodynamic characteristics of arbitrary slender re-entry shapes, J. Spacecraft 3, 247, 1966.

26. L.N. Trefethen, Numerical computation of the Schwarz-Christoffel transformation, Stanford U. Rep. STAN-CS-79-710, 1979.

27. V.J. Rossow, Conformal mapping for potential flow about airfoils with attached flap, J. Aircraft 10, 60, 1973.

28. G. Moretti, A numerical analysis of muzzle blast precursor flow, POLY M/AE Rep. 80-10, 1980.

29. H. Kober, Dictionary of conformal representations, Dover Publ., New York, 1952.

30. D.A. Caughey and A. Jameson, Accelerated iterative calculation of transonic nacelle flowfields, AIAA J. 15, 1474, 1977.

31. B.G. Arlinger, Calculation of transonic flow around axisymmetric inlets, AIAA J. 13, 1614, 1975.

32. D.C. Ives, A modern look at conformal mapping, including multiply connected regions, AIAA J. 14, 1006, 1976.

33. R.G. Legendre, Work in progress in France related to computation of profiles for turbomachine blades by hodograph method, ASME Paper 72-gt-41, 1972.

34. D.C. Ives and J.F. Liutermoza, Analysis of transonic cascade flow using conformal mapping and relaxation techniques, AIAA J. 15, 647, 1977.

35. D.A. Frith, Inviscid flow through a cascade of thick, cambered airfoils, ASME Papers 73-gt-84 and 73-gt-85, 1973.

36. G. Moretti, Computation of shock layers about ablated, blunt-nosed bodies, POLY Rep. 77-14, 1977.

37. D.W. Hall, Calculation of inviscid supersonic flow over ablated nosetips, AIAA Paper 79-0342, 1979.

0., .2, 1.02

0., 0., 1.4

-.2, 0., 1.2

.9, 2.5, 3.15

-.2, .2, 1.2165

1.5, 2.5, 3.7
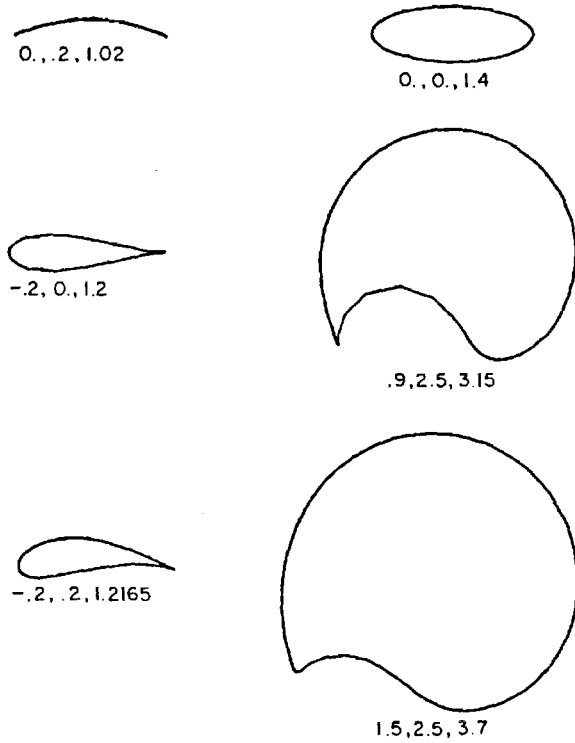
Figure 1.- Joukowski contours for different values
of Real(c), Imag(c), r.

A'   A

B'   B

C'   C

D'   D

E'   E
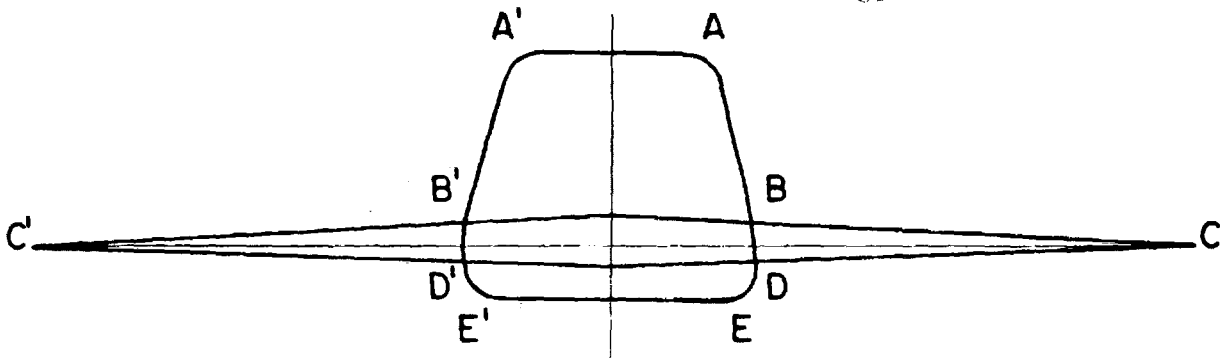
Figure 2.- Cross-section of fuselage and wing.
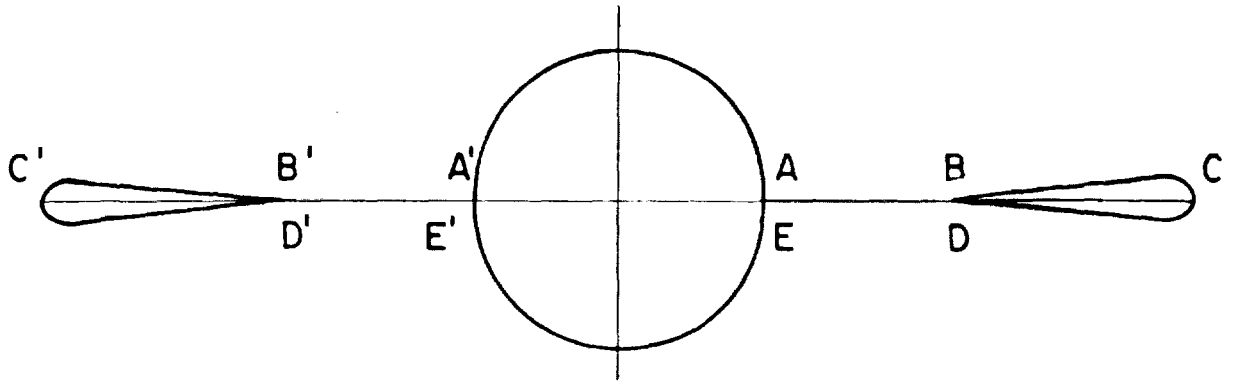
Figure 3.- Cross-section of fuselage and arrow wing.
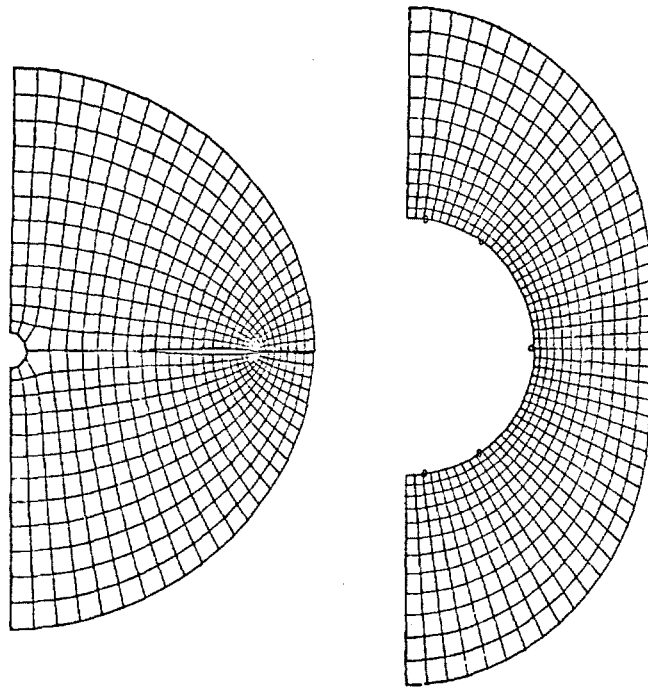
Figure 4.- Grid for fuselage-and-arrow-wing calculation,
in physical plane and mapped plane.
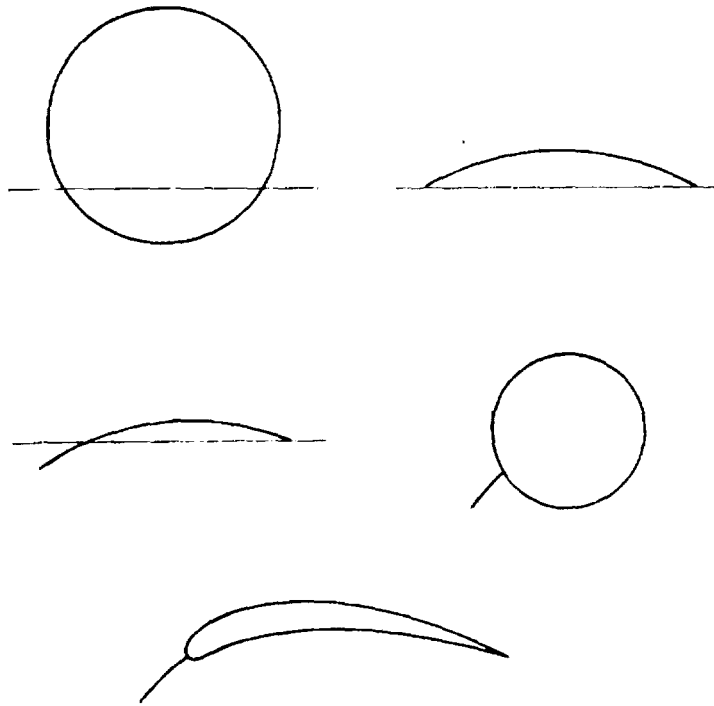
Figure 5.- Generation of wing with attached flap.
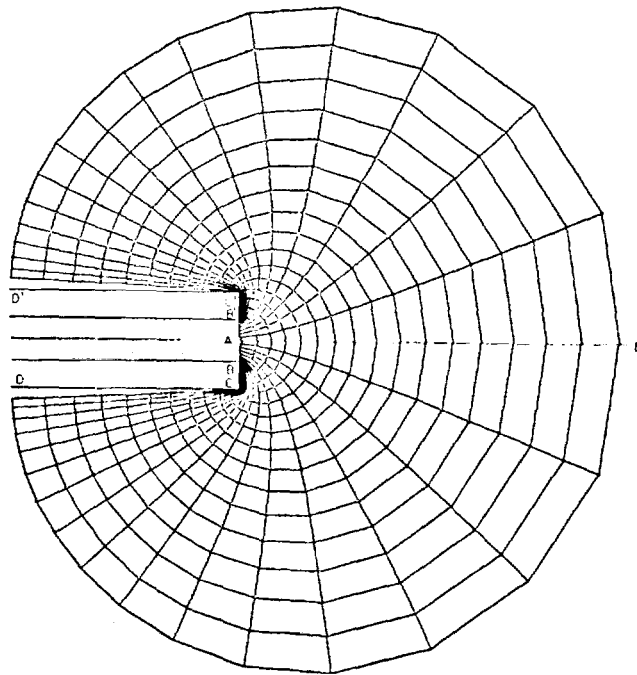
Figure 6.- Grid for muzzle blast calculation.

27
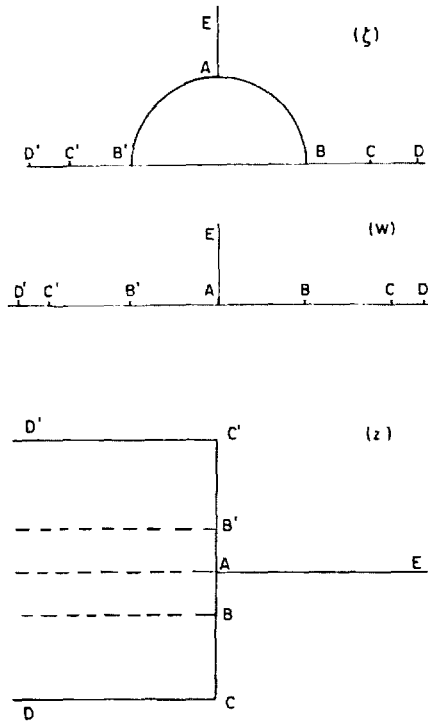
Figure 7.- Generation of the muzzle mapping.
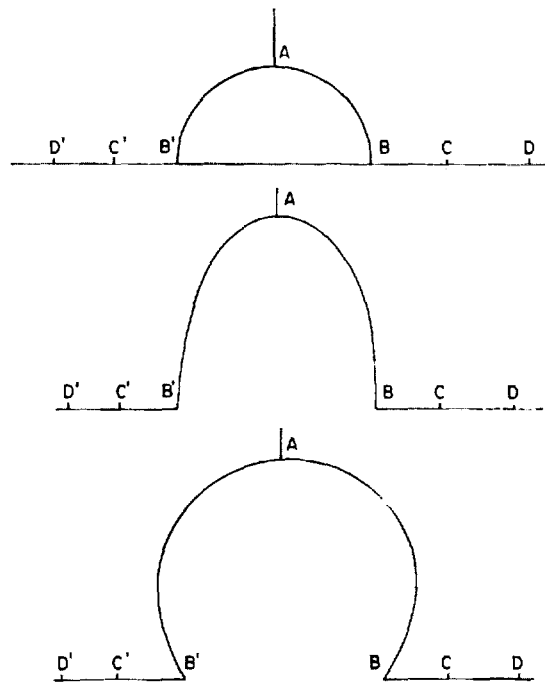
Figure 8.- Generation of the muzzle mapping,
with protruding bullet.
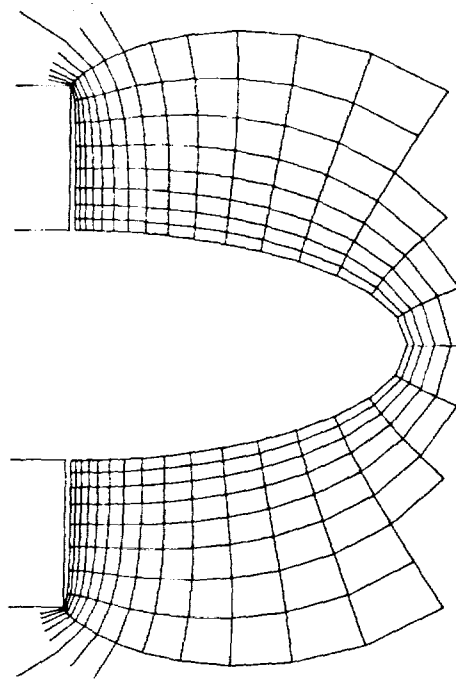
Figure 9.- Grid for muzzle with
protruding bullet.
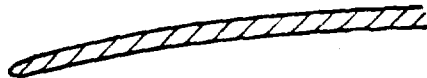
Figure 10.- Nacelle geometry.
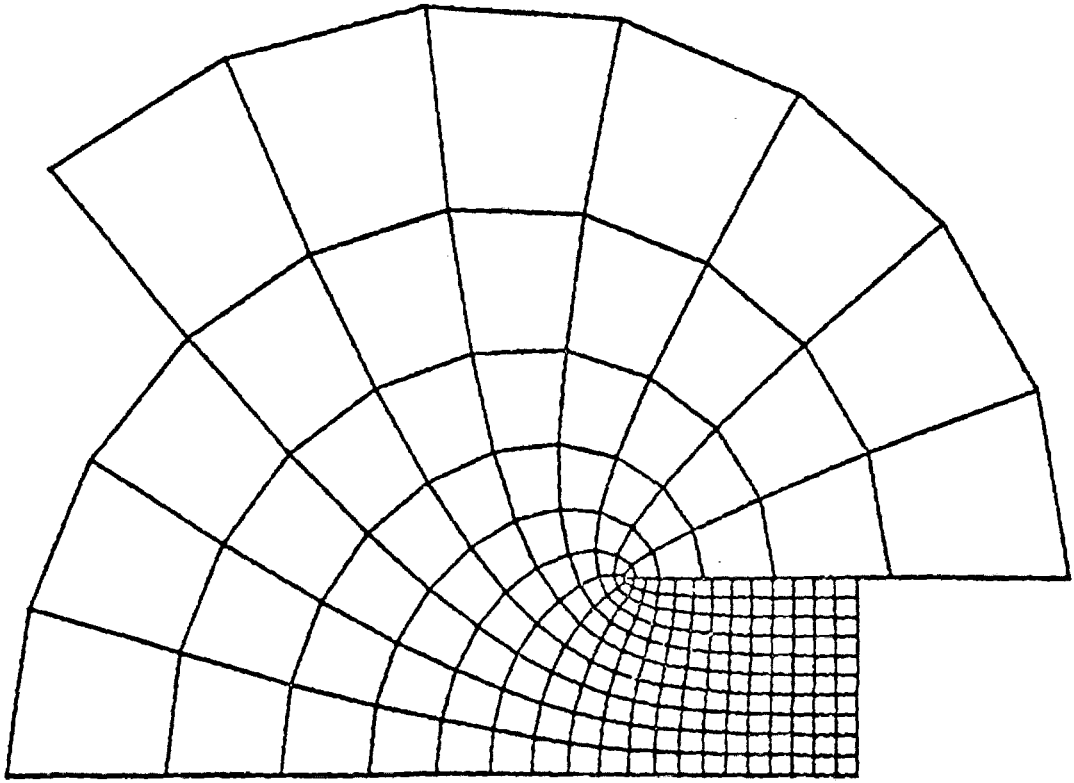
Figure 11.- Grid generated by equation (16).
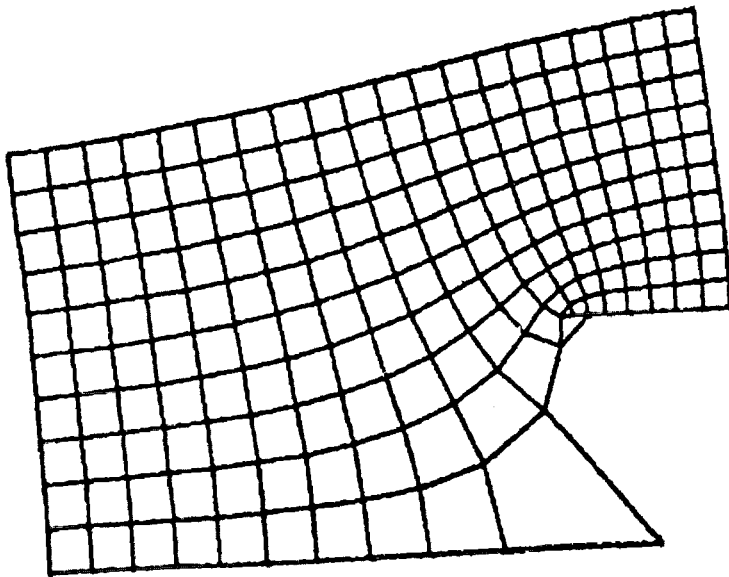
Figure 12.- Grid generated by equation (17),
Cartesian coordinates.
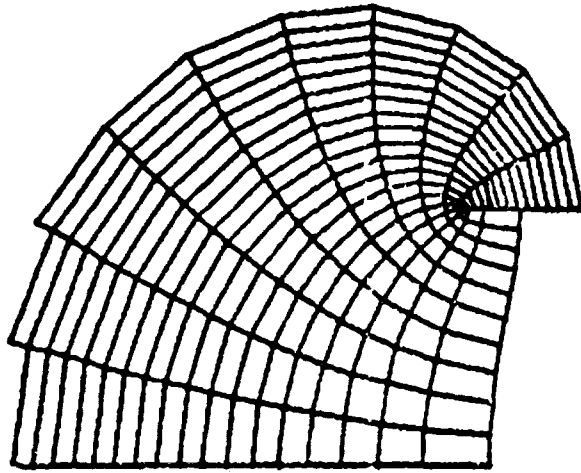
Figure 13.- Grid generated by equation (17),
polar coordinates.
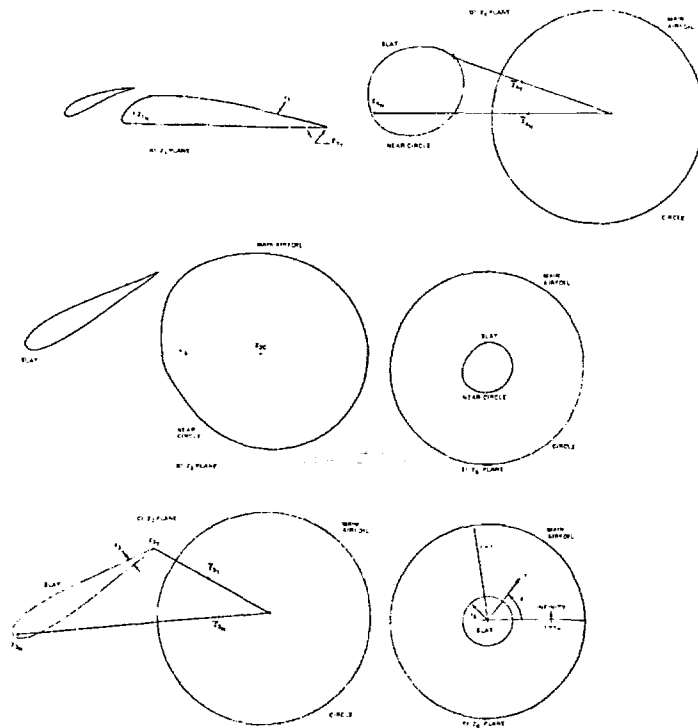
Figure 14.- Mapping of two airfoils onto
two concentric circles.
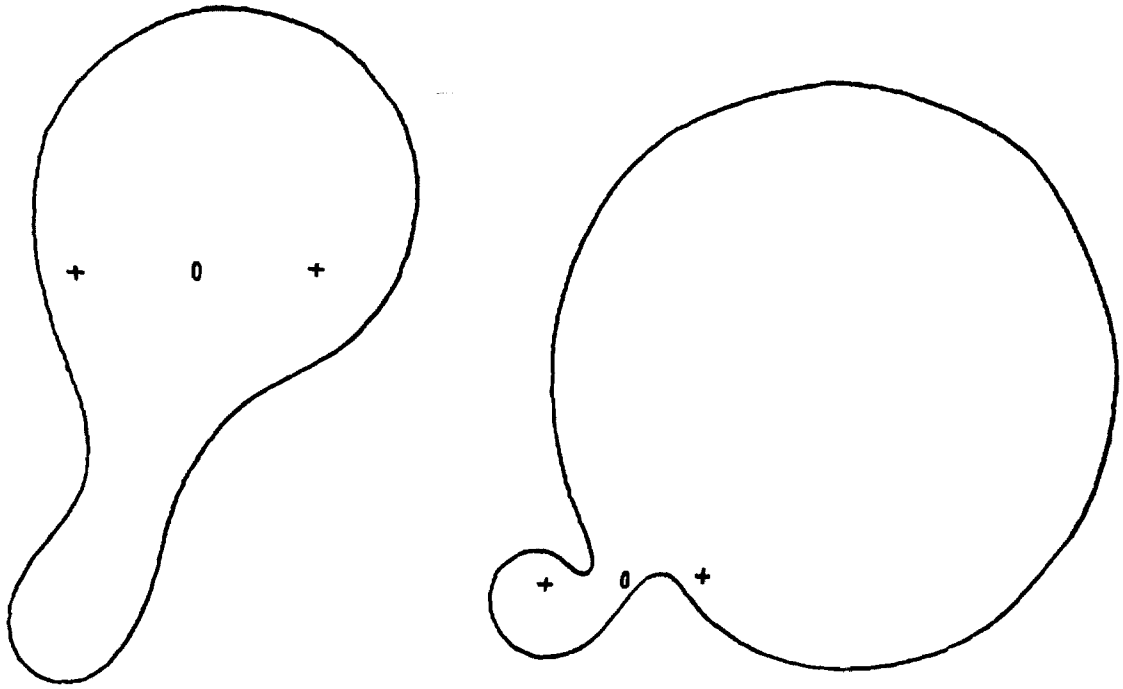
Figure 15.- "Quasi-circles" mapped from cascades of high solidity.
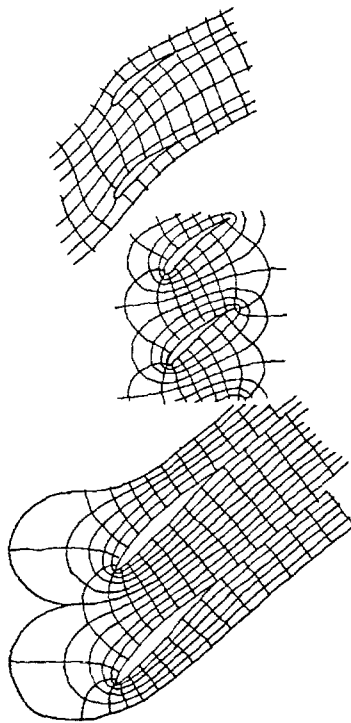
Figure 16.- Different grids for cascades.
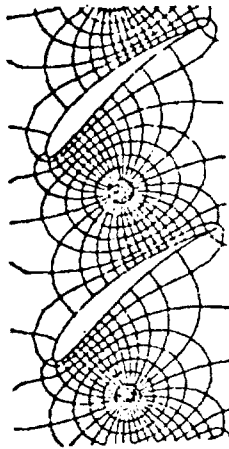
Figure 17.- Frith's grid for cascades.
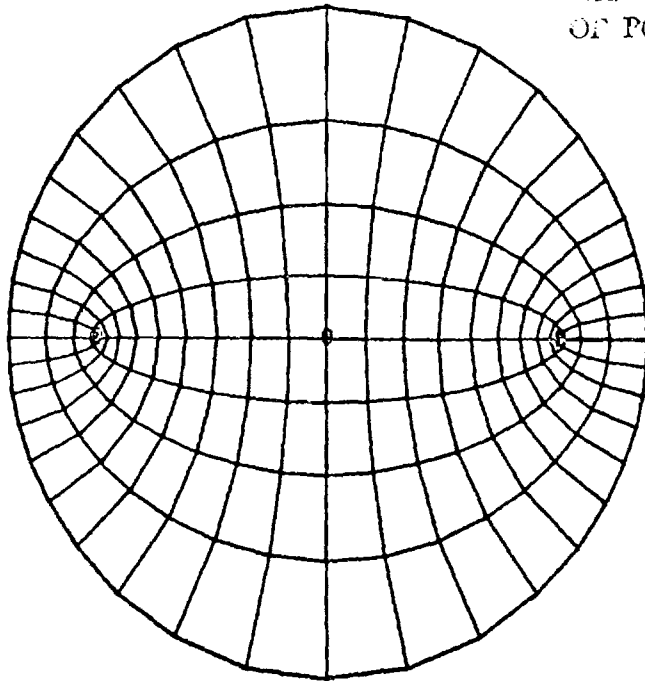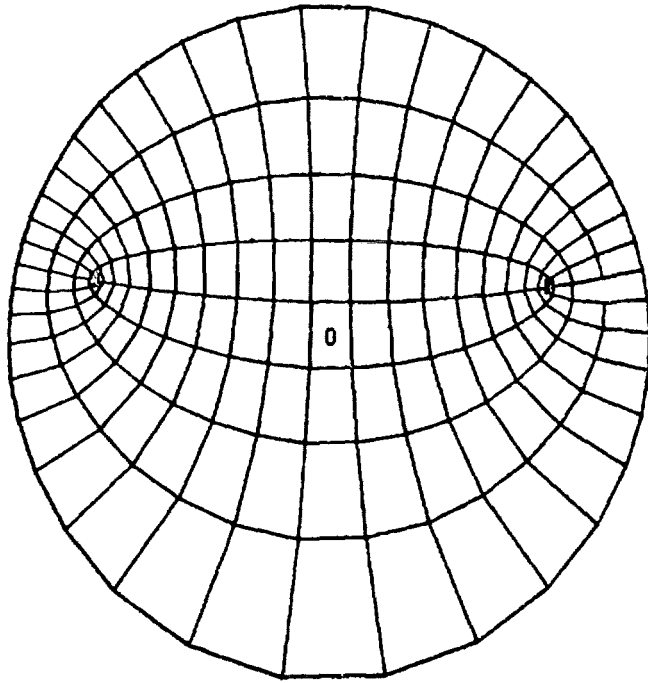
Figure 18.- Circle mapped from rectangle,
equation (25).

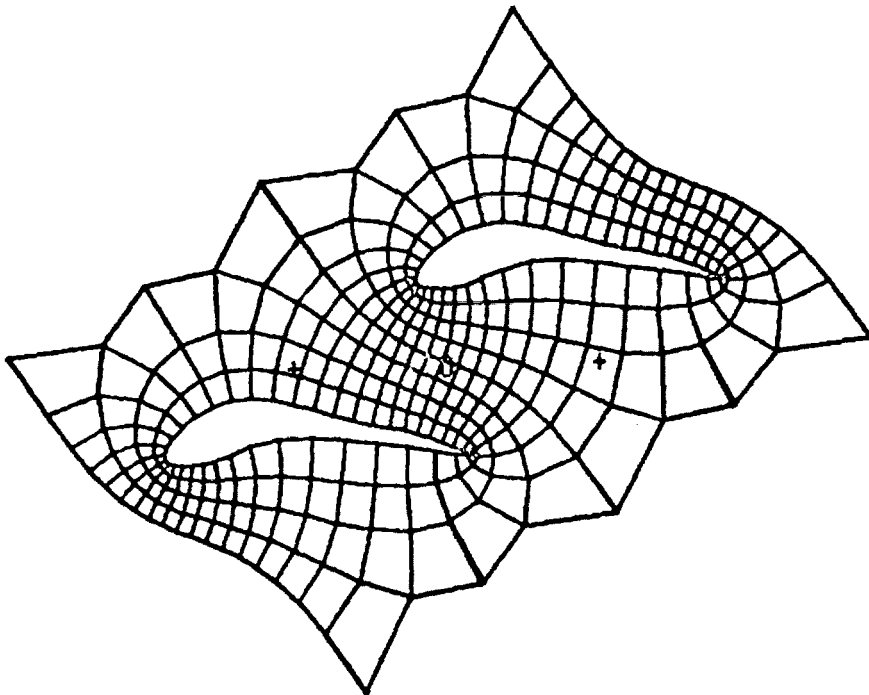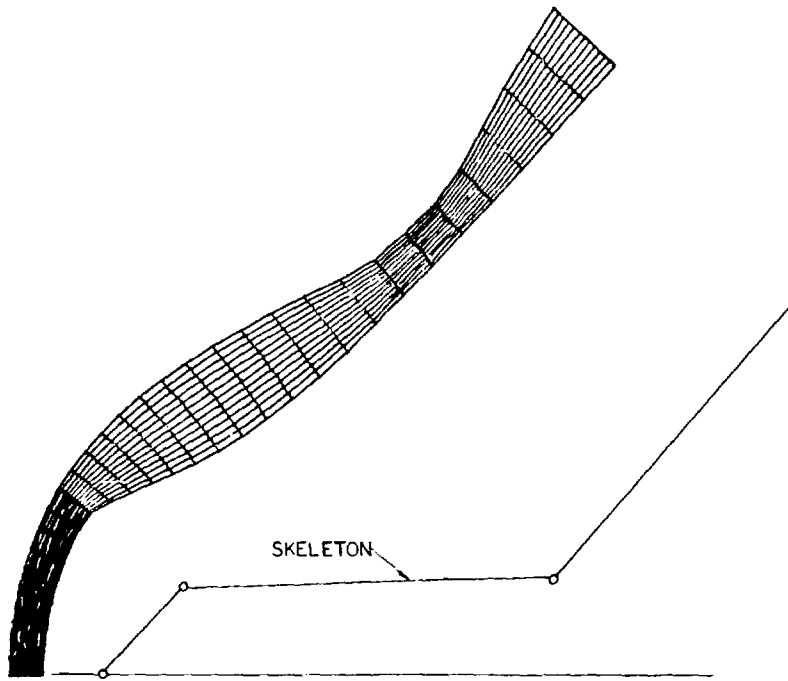Figure 19.- Circle mapped from cascade, equation (20).

Figure 20.- Cascade obtained from circle of Figure 19.

Figure 21.- Grid for ablated body.